Eur. Phys. J. B **59**, 185–192 (2007)
DOI: 10.1140/epjb/e2007-00274-4

THE EUROPEAN PHYSICAL JOURNAL B

Quantum diffusion in polaron model of poly(dG)-poly(dC) and poly(dA)-poly(dT) DNA polymers

H. Yamada[1,a], E.B. Starikov[2,b], and D. Hennig[3,c]

[1] Yamada Physics Research Laboratory, Aoyama 5-7-14-205, Niigata 950-2002, Japan
[2] Institut für Nanotechnologie Forschungszentrum Karlsruhe Postfach3640, 70621 Karlsruhe, Germany
[3] Humboldt Universität zu Berlin, Institut für Physik, Newtonstr. 15, 12489 Berlin, Germany

Received 20 May 2007
Published online 10 October 2007 –

Abstract. We numerically investigate quantum diffusion of an electron in a model of poly(dG)-poly(dC) and poly(dA)-poly(dT) DNA polymers with fluctuation of the parameters due to the impact of colored noise. The randomness is introduced by fluctuations of distance between two consecutive bases along the stacked base pairs. We demonstrate that in the model the decay time of the correlation can control the spread of the electronic wavepacket. Furthermore it is shown that in a motional narrowing regime the averaging over fluctuation causes ballistic propagation of the wavepacket, and in the adiabatic regime the electronic states are affected by localization.

PACS. 87.15.-v Biomolecules: structure and physical properties – 63.20.Kr Phonon-electron and phonon-phonon interaction

1 Introduction

Charge transfer/transport properties in DNA attract lively interest among physicists, chemists and engineers [1–9]. It is now well established that diverse DNA structural deformations are of extreme importance during the charge transfer/transport process, because they help to create polarons which promote not only the formation of a localized electronic state, but may also assist in rendering the latter mobile [10]. Remarkably, recent sophisticated experimental techniques, like, for example, spin-echo spectroscopy, allow to measure stochastic structural dynamics of monomers in polymer chains, such as double-stranded DNA [11–13]: there is a wealth of dynamical modes possessed of a quasi-continuum spectrum. In principle, each of these can influence DNA charge transfer/transport, but, since there are more or less active modes [14], it is possible to take the whole manifold of DNA molecular vibrations into two parts – those which are most active, plus a "stochastic bath" consisting of all other ones. For the present, a number of the polaron models have been proposed to describe charge transfer/transport in DNA polymers, see, for example, [10,15–19]. On the other hand, computer simulations have pinpointed the crucial significance of dynamical disorder for DNA transfer/transport [21–25], and several attempts to formulate stochastical models for the interplay of the former and the latter have already appeared in the literature, see, for example, [26,27].

In this communication, we shall deal with the polaron-like model by Hennig and coworkers as described in the works [16,17], where charge+breather propagation along DNA homopolynucleotide duplexes, i.e. in the both poly(dG)-poly(dC) and poly(dA)-poly(dT) DNA polymers has been studied. These works find that the coupled motion of charges and breathers connected with localized structural vibrations may contribute to highly efficient long-range conductivity.

In our previous paper, we have investigated localization properties of electronic states in the adiabatic limit using a stochastic-bond-vibration approach for poly(dG)-poly(dC) and poly(dA)-poly(dT) DNA polymers within the framework of the polaron model [20]. That time, we assumed that the disorder is caused by DNA vibrational modes, and it influences the charge transfer/transport along DNA duplexes via electron-vibrational coupling. Here we present numerical results concerning the influence of stochastic changes in DNA hydrogen-bond stretchings and double-helical twisting angles, as well as the effects of finite system size, on the electron localization properties.

Specifically, in the present paper we numerically investigate quantum diffusion of electron in the Hennig model of poly(dG)-poly(dC) and poly(dA)-poly(dT) with added fluctuations. The latter are described by a colored noise associated with stochastic dynamics of the

[a] e-mail: hyamada@uranus.dti.ne.jp
[b] e-mail: starikow@chemie.fu-berlin.de
[c] e-mail: hennigd@physik.fu-berlin.de

distances $r(t)$ between two Watson-Crick base pair partners: $\langle r(t)r(t^{'})\rangle = r_0^2 \exp(-|t-t^{'}|/\tau)$. These fluctuations can be regarded as a stochastic process at high temperature, with phonon modes being randomly excited. In the model the characteristic decay time τ of the correlation can control the spread of the electronic wavepacket. Interestingly, the white-noise limit $\tau \to 0$ can in effect correspond to a sort of motional narrowing regime, (see, for example, [28]) because we find that such a regime causes ballistic propagation of the wavepacket through homogeneous DNA duplexes. Still, in the adiabatic limit $\tau \to \infty$, DNA electronic states should be strongly affected by localization.

The amplitude r_0 of the random fluctuations within the base pairs (the fluctuation of the distance between two bases in a base pair) and the correlation time τ, are very critical parameters for the diffusive properties of wavepackets. The finding of ballistic behavior in the white-noise limit vs. localization in the adiabatic limit is interesting, since there is a number of experimental works [29–31] observing ballistic conductance of DNA in water solutions, which is also temperature-independent [31]. Zalinge et al. have tried to explain the latter effect, using a kind of acoustic phonon motions in DNA duplexes [31], which seems to be plausible [32], but not the only possible physical reason. We will propose an alternative explanation for the observed temperature-independent conductance, based upon our numerical results.

The outline of the present paper is as follows. In the next section we introduce our DNA model for the investigation of its diffusive electronic properties. In Section 3, we give a brief explanation for the characteristic motion of wavepackets under the impact of colored noise. In Section 4 we present numerical results concerning the influence of the hydrogen-bond stretching fluctuations and twist angles on the localization properties. Furthermore we comment on the relation between our numerical result and the experimental one. The last section contains our conclusions.

2 Model and parameters

The Hamiltonian for the electronic part in our DNA model is given by

$$H_{el} = \sum_n E_n C_n^\dagger C_n - \sum_n V_{nn+1}(C_n^\dagger C_{n+1} + C_{n+1} C_n^\dagger), \quad (1)$$

where C_n and $C_n^\dagger$ are creation and annihilation operators of an electron at the site n. The on-site energies E_n are represented as

$$E_n = E_0 + k r_n, \quad (2)$$

where E_0 is a constant and r_n denotes the structural fluctuation caused by the coupling with the transversal Watson-Crick H-bonding stretching vibration.

The transfer integral V_{nn+1} depends on the three-dimensional distance d_{nn+1} between adjacent stacked base pairs, labeled by n and $n+1$, along each strand – and is expressed as follows,

$$V_{nn+1} = V_0(1 - \alpha d_{nn+1}). \quad (3)$$

The parameters k and α describe the strength of the interaction between the electronic and vibrational variables. The 3D displacements d_{nn+1} bring about also a variation of the distances between neighboring bases along each strand. The first order Taylor expansion around the equilibrium positions is given by

$$d_{nn+1} = \frac{R_0}{\ell_0}(1 - \cos\theta_0)(r_n + r_{n+1}). \quad (4)$$

R_0 represents the equilibrium radius of the helix, θ_0 is the equilibrium double-helical twist angle between base pairs, and ℓ_0 the equilibrium distance between bases along one strand given by

$$\ell_0 = (a^2 + 4R_0^2 \sin^2(\theta_0/2))^{1/2}, \quad (5)$$

with a being the distance between neighboring base pairs in the direction of the helix axis. We adopt realistic values of the parameters obtained from the semi-empirical quantum-chemical calculations [33]. (See Tab. 1.)

Table 1. Basic parameters for DNA molecules. The subscripts, AT and GC, for k and α denote for ones of the poly(dA)-poly(dT) and poly(dG)-poly(dC) DNA polymers, respectively.

parameter	*value*
E_0	0.1 [eV]
V_0	0.1 [eV]
a	3.4 [Å]
R_0	10 [Å]
θ_0	36 [°]
k_{AT}	0.778917 [eV Å^{-1}]
α_{AT}	0.053835 [Å^{-1}]
k_{GC}	–0.090325 [eV Å^{-1}]
α_{GC}	0.383333 [Å^{-1}]

The Schrödinger equation describing the temporal evolution of the electron state vector $|\psi\rangle$ reads

$$i\hbar \frac{\partial|\psi\rangle}{\partial t} = H_{el}(t)|\psi\rangle. \quad (6)$$

The explicit time-dependence of the Hamiltonian $H_{el}(t)$ is given through both the time-dependence of the on-site and hopping terms. The equation can be expressed by scaled dimensionless variables as,

$$i\hbar_{eff} \frac{\partial \phi_n}{\partial t} = E_n(t)\phi_n - V_{nn+1}(t)\phi_{n+1} - V_{n-1n}(t)\phi_{n-1}, \quad (7)$$

where $\phi_n = \langle n|\psi\rangle$ and the effective Planck constant $\hbar_{eff} = 0.53$. We redefined the scaled dimensionless variables $E_n(t)$ and $V_{nn+1}(t)$ in equation (1), as $\frac{E_n}{V_0} \to E_n$, $\frac{V_{nn+1}}{V_0} \to V_{nn+1}$.

In addition to the DNA homopolymer duplexes, we also investigate the mixed sequence consisting of two

types of the Watson-Crick pairs. Then, as a zero-order approximation, the electron-phonon coupling parameters for the mixed GC/AT stacks are taken here to be equal to the values obtained for poly(dG)-poly(dC) and poly(dA)-poly(dT) DNA polymers.

We used mainly 4th order Runge-Kutta-Gill method in the numerical simulation for the time evolution with time step $\delta t = 0.01$. In some cases we confirmed the accuracy of the so obtained results by complete accord with the results gained with the help of a 6th order symplectic integrator that is higher order unitary integrations.

3 Fluctuation of the $r_n(t)$ and motion of wavepackets

The explicit time-dependence of the Hamiltonian comes from the fluctuation of the variable $r_n(t)$ at each site n. To mimic these fluctuations we use a Gaussian-Markovian process with standard deviation r_{n0}(amplitude) and correlation time τ characterized by the following covariance

$$C(t-t^{'}) \equiv \langle r_n(t) r_m(t^{'})\rangle = \delta_{nm} r_{n0}^2 e^{-|t-t^{'}|/\tau}, \quad (8)$$

where $\langle r_n(t)\rangle = 0$. This process is called the Ornstein-Uhlenbeck process. There is no spatial correlation, viz., the stochastic fluctuations at different sites are independent of each other. The white-noise limit corresponds to $\tau \to 0$. On the other hand, the adiabatic limit ($\tau \to \infty$) corresponds static Anderson model. A numerical way for the generation of the colored noise is given in appendix A. The fluctuations are characterized by two parameters, i.e. amplitude r_{n0} and correlation time τ. Another relevant quantity is,

$$D_0 \equiv \int_0^\infty C(t)dt = r_{n0}^2 \tau. \quad (9)$$

The quantity D_0 expresses total strength for the random fluctuation and is related to self-diffusion coefficient [34–36]. The limit $\tau \to 0$ and $r_{n0} \to \infty$ with keeping $D_0 = const.$ yields Gaussian white-noise characterized by $\langle r_n(t) r_n(t^{'})\rangle = 2D_0\delta(t-t^{'})$. For $|t-t^{'}|\tau$, we may treat $r_n(t)$ and $r_n(t^{'})$ as statistically independent quantities. This limiting case becomes valid when the lattice temperature is well above the Debye temperature. We set a characteristic decay rate τ_c of the correlation function through,

$$\tau_c = \frac{\hbar\Omega}{V_0} \sim 0.05, \quad (10)$$

where Ω is the frequency of the slow bond vibrations. The scaled dimensionless quantity τ_c means time-scale separation between the fast electron motion and the slow lattice vibrations. The adiabatic limit holds true for $\tau \gg \tau_c$ allowing for the application of the Born-Oppenheimer approximation.

In general, in our numerical simulation, the order of mean values $\langle E_n(t)\rangle, \langle V_{nn+1}(t)\rangle$ and the amplitude of the fluctuations (standard deviation) $\Delta E_n(t), \Delta V_{nn+1}(t)$ of the on-site energy and the transfer energy are estimated as follows: $\langle E_n(t)\rangle \sim O(1), \Delta E_n(t) \sim k r_{n0}, \langle V_{nn+1}(t)\rangle \sim O(1), \Delta V_{nn+1}(t) \sim 2\alpha r_{n0} F_0$, where $F_0 \equiv \frac{R_0}{\ell_0}(1-\cos\theta_0)$. As the fluctuating amplitude is concerned it can be naturally incorporated by assuming the temperature dependence as,

$$r_{n0}^2 \propto k_B T, \quad (11)$$

Particularly, at room temperature, i.e. for $k_B T = 0.026$ [eV], the value of the scaled dimensionless thermal energy is given by $k_B T/V_0 = 0.26$.

The motion of the electron in the fluctuating medium is crucially influenced by the values of the parameters r_{n0} and τ. Another important parameter is the band width B of the electron system which is given by the static case without fluctuation $r_{n0} = 0$. In the scaled Hennig model for DNA the band width is $B \sim 2$, although the exact value depends on A-T or G-C or mixed models. In order to infer on the consequences of the noise for the elelctron-motion it illustratitive to express the parameters of the noise in units of r_{n0}. Thus, with regard to its influence on the motion the noise is quantified by the effective parameters B/r_{n0} and $1/(\tau r_{n0})$. While B and $1/\tau$ have the effect of narrowing the absorption linewidth, r_{n0} has the opposite effect, namely broadening of the linewidth. The motional narrowing of the resonant absorption linewidth becomes important when the fluctuation rate is larger than the amplitude, i.e. $\tau^{-1} > r_{n0}$. It then follows that time-dependent perturbation theory is true for $B/r_{n0} \gg 1$ or $1/(\tau r_{n0}) \gg 1$, and the adiabatic approximation is applicable in the region $\tau B \gg 1$. In the following sections we show some typical wavepacket dynamics in the different parameter regimes.

Note that the ballistic propagation of a wave packet occurs when $\tau \leq \delta t (= 0.01)$, i.e. the fluctuation is very rapid and the system is reduced to a regular system without any disorder.

4 Numerical results

In this section, we show the numerical results of the wavepacket dynamics. We consider quantum diffusion of an initially localized wavepacket $\phi_n(t=0) = \delta_{nn_0}$. Then we mainly monitor the time-dependence of the mean square displacement (MSD)

$$m(t) = \sum_n^N \langle \phi_n | (\hat{n} - n_0)^2 | \phi_n \rangle, \quad (12)$$

and the distribution function $P(n,t) \equiv |\langle n|\psi(t)\rangle| = |\phi_n(t)|$. We used $N = 2^{12}$ and $n_0 = N/2$ through this paper.

4.1 Constant hopping term $V_{nn+1} = 1 (\alpha = 0)$

First we present our numerical results of simple cases with a constant transfer integral $V_{nn+1} = 1.0$ for all n.

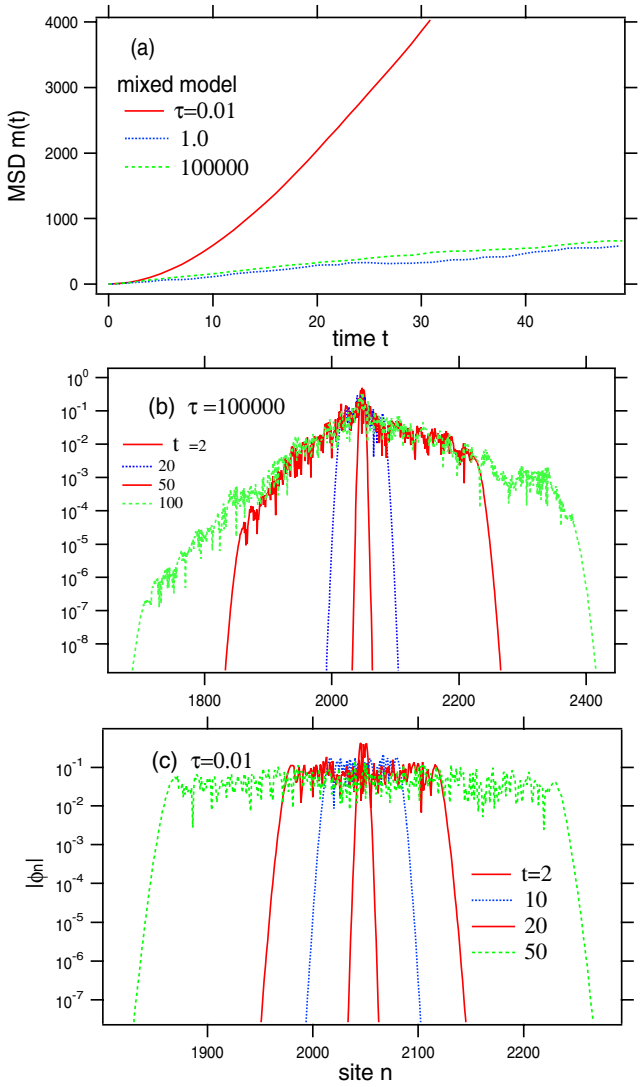

Fig. 1. (a) $m(t)$ at cases with $\tau = 0.001, 1, 100000$ in the mixed model with a constant hopping $V_{nn+1} = V_0 = 1.0$. Some snapshots of $|\phi_n(t)|$ at $t = 2, 20, 50, 100$ in the case with $\tau = 10^5$(b) and $\tau = 0.01$(c).

We illustrate the typical motion of a wavepacket in cases when only the on-site energy $E_n(t)$ fluctuates according to a Ornstein-Uhlenbeck process. Although we used mixed model in this case the qualitative result does not depend on the type of model even if we adapt A-T model and G-C model.

Figure 1a shows time-dependence of the MSD for various correlation times $\tau = 10^5, 1, 0.01$ at $r_{n0} = 1.0$. In Figure 1b and c we depict some snap-shots of $|\phi_n(t)|$ in cases with $\tau = 0.01$ and $\tau = 10^5$, respectively. In the case $\tau = 0.01$, $m(t)$ shows ballistic behavior ($m(t) \sim t^2$) which is due to "motional narrowing" caused by the short-time correlation. On the other hand, in the case $\tau = 10^5$ $m(t)$ shows typical localization behavior within this time scale due to Anderson localization. In the intermediate

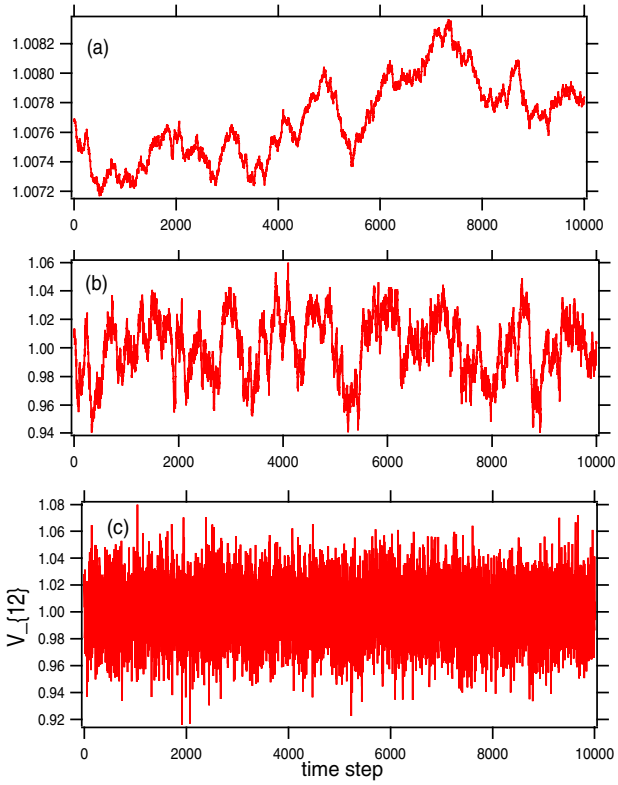

Fig. 2. The time-dependence of the hopping term $V_{12}(t)$ at $n = 2$ in A-T model with $r_{n0} = 1.0$ for various correlation times $\tau = 10^5$(a), $\tau = 1.0$(b), $\tau = 0.01$(c).

case $\tau = 1$, $m(t)$ shows normal diffusion with Gaussian shape.

4.2 Fluctuating hopping term

Next, we show the numerical results of some cases with fluctuating hopping terms $V_{nn+1}(t)$ obeying equation (3). Figure 2 shows some typical time-dependence of the hopping term $V_{12}(t)$ for various correlation times $\tau = 10^5, 1, 0.01$. The latter correspond to adiabatic, intermediate and rapid fluctuations, respectively.

Figure 3 displays the time-dependence of the MSD in A-T, G-C and mixed model with $r_{n0} = 1.0$ for various correlation times $\tau = 10^5, 1, 0.01$. Snap-shots of $|\phi_n(t)|$ in A-T model for various correlation time $\tau = 10^5, 1, 0.01$ are shown in Figure 4. As a result we obtain that the essential behavior does not depend on existence of the fluctuations of the hopping term. The dynamical behavior is qualitatively similar to the cases discussed in the preceding section with constant $V_{nn+1} = 1$. In the relatively short-correlation case (white-noise limit $\tau = 0.01$), the wave packet exhibits ballistic propagation. The extent of the spread of the wavepacket in the A-T model is larger than that of the G-C model. On the other hand, in the adiabatic limit ($\tau = 10^5$) the wave packet localizes, which corresponds to Anderson localization. The localization length is $\ell \sim 20$ sites. It seems that the localization

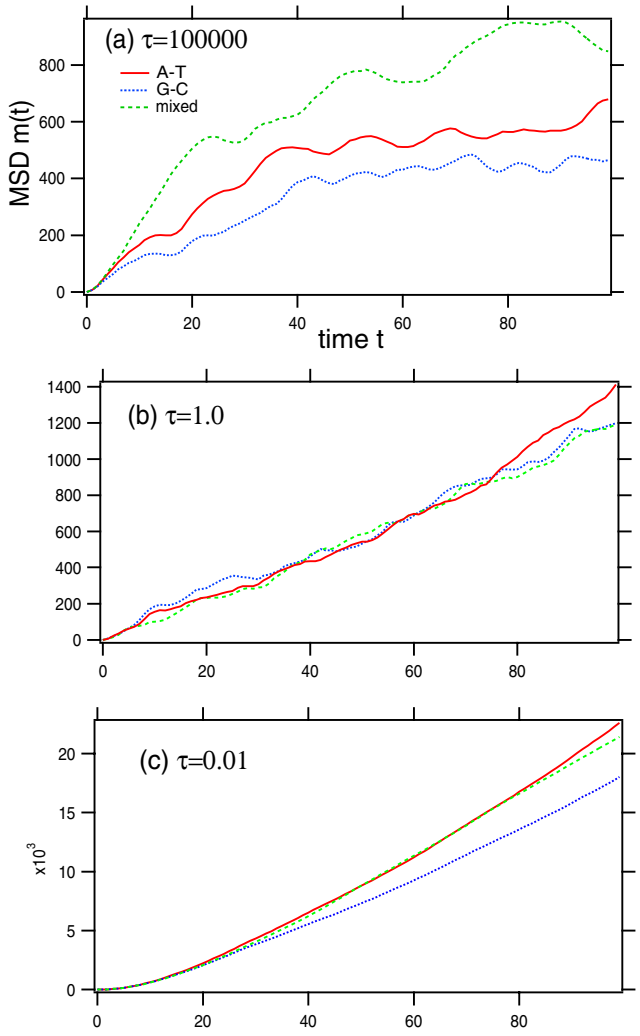

Fig. 3. $m(t)$ in A-T, G-C, and mixed models with $r_{n0} = 1.0$ and $\tau = 10^5$(a), $\tau = 1.0$(b), $\tau = 0.01$(c).

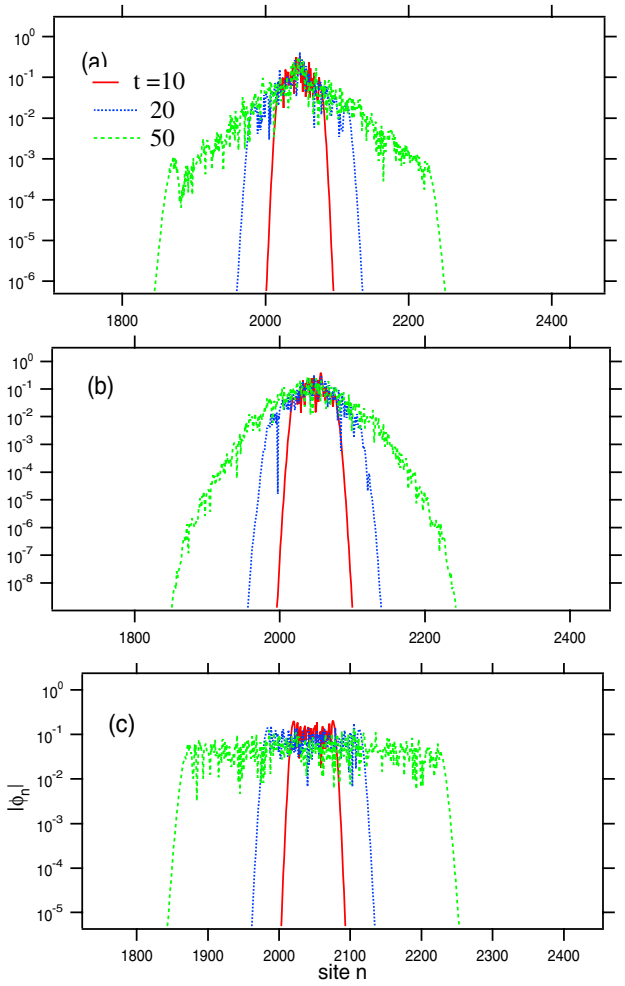

Fig. 4. Some snap shots of $|\phi_n|$ at $t = 10, 20, 50$ in the A-T model with $r_{n0} = 1.0$ and $\tau = 0.01$(a), $\tau = 1$(b), $\tau = 10^5$(c).

length of the A-T model is slightly larger than that of the G-C model on this scale.

Next in Figure 5 we show a typical MSD and $P(n,t)$ for the relatively small fluctuation strength $r_{n0} = 0.1$ in the mixed model with $\tau = 1$. As evident from the relation in equation (9), in comparison to the case with a comparatively large fluctuation amplitude $r_{n0} = 1.0$ (cf. Fig. 3b) for a smaller amplitude $r_{n0} = 0.1$ the quantum diffusion behaves ballistically ($m \sim t^2$) within the same time scale. For the $A-T$ and the $G-C$ model we found similar behavior in dependence on the change in the fluctuation strength r_{n0}.

4.3 Diffusion rate

Here we investigate the temporal diffusion rate defined as

$$D(t) = \frac{\langle m(t) \rangle}{t} \qquad (13)$$

in the almost diffusive range $0.1 < \tau < 10$, where $\langle ... \rangle$ expresses the average over several samples. If the motion of the wave packet is diffusive the diffusion rate is supposed to attain a constant value. Figure 6 shows the diffusion rate as a function of $1/\tau$ for various fluctuation amplitudes r_{n0} in A-T and G-C models. For the estimate of the diffusion rate we used a time interval $t = 10^5 \delta t$. where the error of the diffusion rate is less than ten percent. $D(t)$ approaches zero for adiabatic limit ($\tau \gg 1$) due to Anderson localization, while $D(t)$ goes to infinity for motional narrowing case ($\tau \ll 1$). As indicated in Section 3, increase of r_{n0} means increase of temperature. It follows that the diffusion rate in the A-T model is larger than that in G-C model at the relatively low temperature ($r_{n0} = 1$). However, at higher temperatures ($r_{n0} = 3, 5$) the two models exhibit virtually equal behavior in this correlation-time range. Furthermore, in the high-temperature regime there seem to be no pronounced alterations of the diffusion coefficient as a function of τ^{-1}.

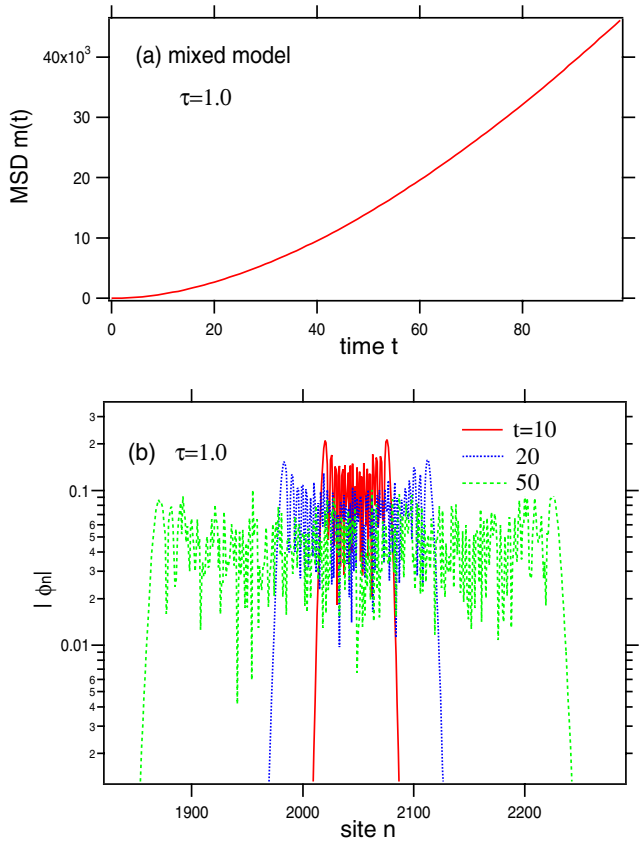

Fig. 5. (a) $m(t)$ and (b) $|\phi_n|$ at $t = 10, 20, 50$ in the mixed model with $r_{n0} = 0.1, \tau = 1$.

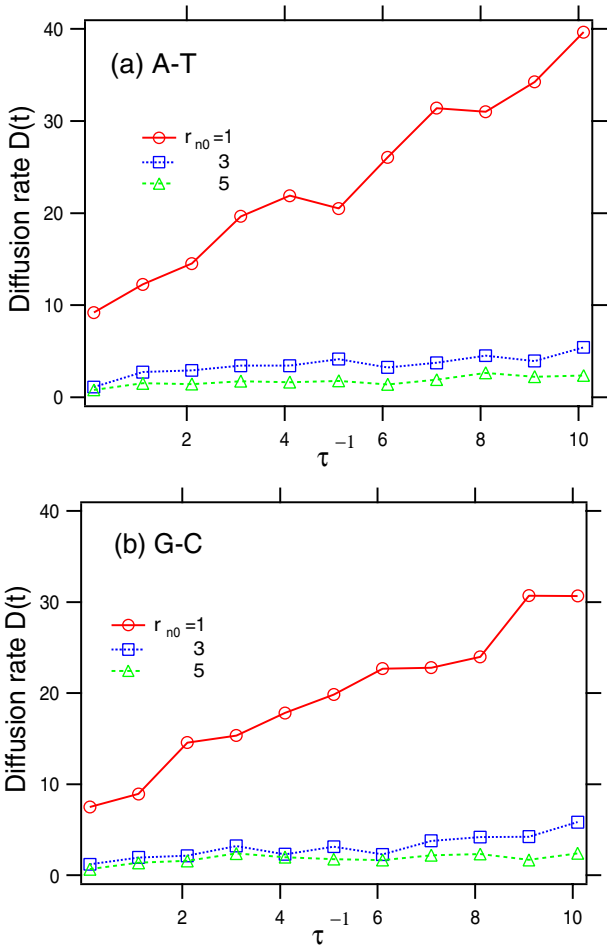

Fig. 6. Diffusion rate $D(t)$ as a function of τ^{-1} for several fluctuation strengths $r_{n0} = 1, 3, 5$ at A-T model(a) and G-C model(b), respectively

4.4 Comparison with experimental results

As mentioned in the introduction, in experiments concerning the temperature effect on the single-molecule conductance of double-stranded oligo-DNA with homogeneous base-pairs Zalinge et al. [31] found temperature-independent ballistic conductance. Furthermore, it has been shown that $(dG)_{15} - (dC)_{15}$ is a better conductor than $(dA)_{15} - (dT)_{15}$ in the conducting experiments, just in accordance with the earlier experimental and theoretical findings [33]. The work [31] explained the observed temperature independence by deactivation of the acoustic modes of DNA at room and higher temperatures.

It is interesting to recall in this context an earlier work [37], where almost temperature independent photoinjected electron/hole mobility has been calculated on the basis of the stochastic Haken-Strobl-Reinecker (HSR) model for discotic liquid crystals. Unlike in our model, the HSR Hamiltonian used in [37] treats all the vibrational and lattice modes as a source of fluctuations of the parameters of the tight-binding model, without singling out any mode responsible for polaron formation. As a result, the HSR mobility temperature independence shows up only at small fluctuations of the molecules around their equilibrium positions. This is not the case in our present model.

We have to pay attention to relatively short-time behavior and/or small spread regime ($\sqrt{m} \sim 15$), as we compare the experimental result with our numerical results. Figure 7 shows the MSD in the A-T model with $\tau = 0.01$ and $\tau = 0.0001$ respectively in which cases ballistic propagation is observed due to the motional narrowing. In the short-time regime the time dependence of the MSD shows relatively weak $\tau-$dependence once the motional narrowing has affected the diffusive behavior. Therefore, the temperature-independence may be caused by the motional narrowing and the finite-size effect in the experiment.

Figure 8 shows the short-time behavior of the cases $\tau = 1$ and $\tau = 0.01$ depicted on a larger time scale in Figure 3. It follows that in the short-time behavior the $(dG)_{15} - (dC)_{15}$ case is more diffusive than its $(dA)_{15} - (dT)_{15}$ counterpart within the range fro which the spread of the wavepacket is $\sqrt{m} \sim 15$.

5 Summary and discussion

We have numerically investigated quantum diffusion of an electron in the Hennig model of poly(dG)-poly(dC) and poly(dA)-poly(dT) DNA polymers with fluctuations

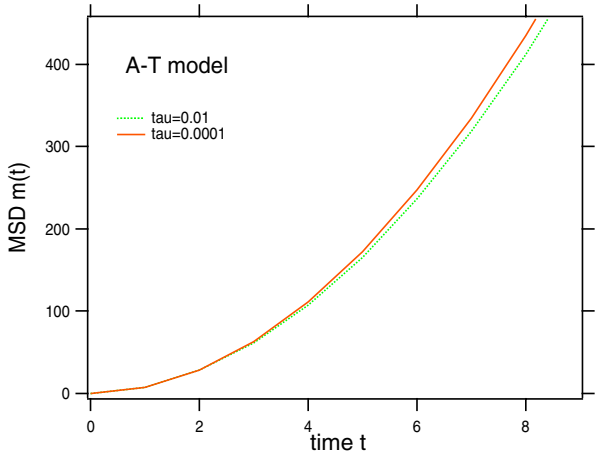

Fig. 7. Short-time behavior of $m(t)$ in the A-T model with $\tau = 0.01, 0.0001$.

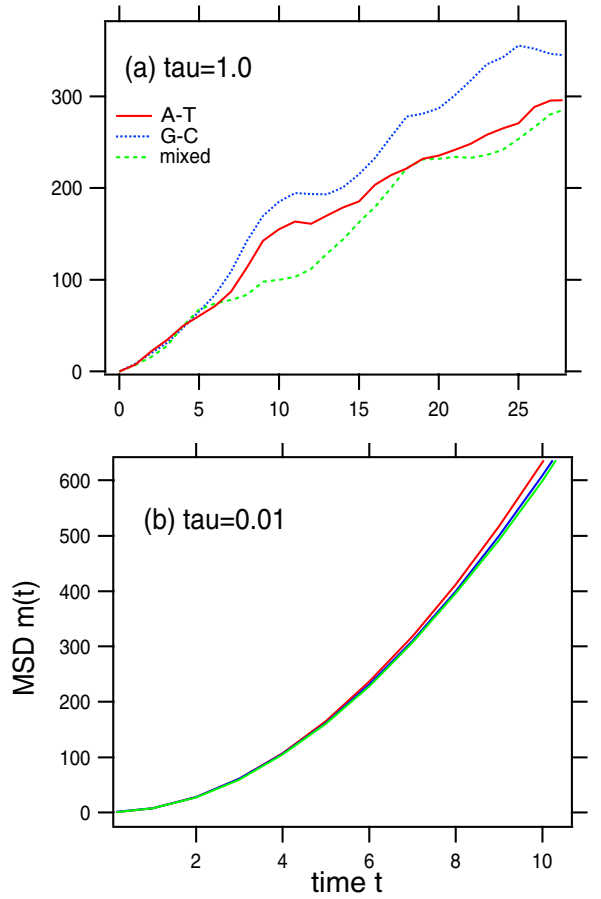

Fig. 8. Short-time behavior of $m(t)$ of A-T, G-C, and mixed models with $r_{n0} = 1.0$ at $\tau = 1$(a) and $\tau = 0.01$(b).

of the parameters caused by colored noise. In the model the decay time of the correlation can control the spread of the electronic wavepacket. It has been shown that in a motional narrowing regime the averaging over fluctuations causes ballistic propagation of the wavepacket and in the adiabatic regime the electronic states are strongly localized. It has been demonstrated that the motional narrowing affects the localization in the poly(dG)-poly(dC) and poly(dA)-poly(dT) DNA polymers. In either model temperature-dependence becomes virtually suppressed when the motion of the wave packet is characterized by ballistic propagation.

We have also investigated the temporal diffusion rate in the almost diffusive range. It has been found that the diffusion rate of the A-T model is larger than that of the G-C model at comparatively low temperatures. Interestingly for relatively high temperatures in the diffusive range of the wavepacket motion the difference between the two DNA systems gets smaller.

Furthermore we commented on the relation between our numerical results and the experimental ones. It was shown that in the short-time behavior the significant difference of the spread of wavepackets does not exist between $(dA)_{15} - (dT)_{15}$ and $(dG)_{15} - (dC)_{15}$ except for the localization cases.

In the present report we used periodic sequences, i.e. constant values of E_0, V_0, as static parts of the on-site and hopping terms for poly(dG)-poly(dC) and poly(dA)-poly(dT) DNA polymers, respectively. This also includes the mixed model. Then the motional narrowing for dynamical disorder makes the time-evolution of the wavepacket ballistic. However, it should be remarked that motional narrowing strongly localizes the wavepacket if we use disordered sequence for the static parts of E_n and/or V_{nn+1}.

We would like to thank Professor Juan F.R. Archilla for discussion in first stage of this work. H.Y. would like to thank Shuichi Kinosita for sending me some related papers.

Appendix A: Generation of colored noise

In this appendix, we give an algorithm in order to generate the Gaussian colored noise $r_n(m\delta t)$ at the mth time step [38]. First, let us assume Gaussian random numbers $z_n(m)$ with zero mean and unit variance at the time $t_m = m\delta t$. Then the stochastic sequence with the colored correlation is obtained by the following recursion:

$$r_n(0) = r_{n0} z_n(0) \tag{14}$$

$$r_n(m) = \rho_m r_n(m-1) + \sqrt{(1-\rho_m^2)}\{r_{n0} z_n(m)\}, \tag{15}$$

where $\rho_0 = 0$, $\rho_m = \exp(-|t_m - t_{m-1}|/\tau)$. Note that index n denotes the site n and m the time step m. In our numerical calculation, $\rho_m = \text{const.}\,(= \exp(-\delta t/\tau))$. We used the algorithm independently for each site n.

It should be noted, that there is another algorithm using the power spectrum of the stochastic process, which is applicable to a lot of types of the correlated sequence [37,39,34–36,40–45].

More recently, it has been shown that motional narrowing due to large thermal fluctuation effects the coherence of relaxation dynamics such as spin relaxation in semiconductors [28] or vibrational dephasing in a spin-Peierls system with lattice fluctuations [46].

References

1. For a recent review, see, for example, D. Porath, G. Cuniberti, R. Di Felice, Top. Curr. Chem. **237**, 183 (2004)
2. P. Tran, B. Alavi, G. Gruner, Phys. Rev. Lett. **85**, 1564 (2000)
3. D.K. Campbell, S. Flach, Y.S. Kivshar, Physics Today, Jan. 43 (2004)
4. Z. Hermon, S. Caspi, E. Ben-Jacob, Europhys. Lett. **43**, 482 (1998)
5. D.N. LeBard, M. Lilichenlo, Yu.A. Berlin, M.A. Ratner, J. Phys. Chem. B **107**, 14509 (2003)
6. S. Roche, Phys. Rev. Lett. **91**, 108101 (2003); S. Roche, D. Bicout, E. Macia, E. Kats, Phys. Rev. Lett. **91**, 22810 (2003)
7. K. Iguchi, Int. J. Mod. Phys. B **17**, 2565 (2003)
8. H. Yamada, Int. J. Mod. Phys. B **18**, 1697 (2004); Phys. Lett. A **332**, 65 (2004)
9. A.V. Malyshev, Phys. Rev. Lett. **98**, 096801 (2007)
10. E.M. Conwell, S.V. Rakhmanova, Proc. Natl. Acad. Sci. USA **97**, 4556 (2000)
11. W. Saenger, *Principles of Nucleic Acid Structure* (Springer, New York, 1984)
12. R. Shusterman, S. Alon, T. Gavrinyov, O. Krichevsky, Phys. Rev. Lett. **92**, 048303 (2004)
13. B.J. Bern, R. Pecora, *Dynamic Light Scattering* (Wiley, New York, 1976)
14. E.B. Starikov, Phil. Mag. **85**, 3435 (2005)
15. E.M. Conwell, D.M. Basko, Synthetic Metals **137**, 1381 (2003)
16. D. Hennig, Euro. Phys. J. B **30**, 211 (2002); D. Hennig, J.F.R. Archilla, J. Agarwal, Physica D **180**, 256 (2003)
17. F. Palmero, J.F.R. Archilla, D. Hennig, F.R. Romero, New J. Phys. **6**, 13 (2004)
18. C. Chang, A.H.C. Neto, A.R. Bishop, Chem. Phys. **115**, 4169 (2004)
19. E.I. Kats, V.V. Lebedev, JETP Lett. **75**, 37 (2002)
20. H. Yamada, E.B. Starikov, D. Hennig, J.F.R. Archilla, Eur. Phys. J. E **17**, 149 (2005)
21. A. Troisi, G. Orlandi, J. Phys. Chem. B **106**, 2093 (2002)
22. S. Tanaka, Y. Sengoku, Phys. Rev., E **68**, 031905 (2003)
23. J.P. Lewis, Th. E. Cheatham, E.B. Starikov, H. Wang, O.F. Sankey, J. Phys. Chem. B **107**, 2581 (2003)
24. A.A. Voityuk, K. Siriwong, N. Roch, Angew. Chem. Int. Ed. **43**, 624 (2004)
25. E.B. Starikov, T. Fujita, H. Watanabe, Y. Sengoku, S. Tanaka, W. Wenzel, Mol. Simul. **32**, 759 (2006)
26. J. Matulewski, S.D. Baranovskii, P. Thomas, Phys. Chem. Chem. Phys. **7**, 1514 (2005)
27. S. Sakamoto, Y. Ohmachi, M. Tomiya, J. Physics: Conf. Series **61**, 1012 (2007)
28. A. Berthelot, I. Favero, G. Cassabois, C. Voisin, C. Delalande, Ph. Roussignol, R. Ferreira, J.M. Gerard, Nature Phys. **2**, 759 (2006).
29. B.Q. Xu, P.M. Zhang, X.L. Li, N.J. Tao, Nano Lett. **4**, 1105 (2004)
30. H. Cohen, C. Nogues, R. Naaman, D. Porath, Proc. Natl. Acad. Sci. USA **102**, 11589 (2005)
31. H. van Zalinge, D.J. Schiffrin, A.D. Bates, E.B. Starikov, W. Wenzel, R.J. Nichols, Angew. Chem. Int. Ed. **45**, 5499 (2006)
32. S.K. Mandal, Appl. Phys. Lett. **89**, 193102 (2006)
33. D. Hennig, E. Starikov, J.F.R. Archilla, F. Palmero, J. Biol. Phys. **30**, 227 (2004)
34. H. Sumi, J. Chem. Phys. **67**, 2943 (1977)
35. Y. Inaba, J. Phys. Soc. Jpn. **50**, 2473 (1981); **52**, 3144 (1983)
36. H. Ezaki, F. Shibata, Physica A **176**, 581 (1991)
37. M.A. Palenberg, R.J. Silbey, M. Malagoli, J.-L. Bredas, J. Chem. Phys. **112**, 1541 (2000)
38. L. Baratosch, Int. J. Mod. Phys. B **12**, 851 (2001)
39. H. Haken, G. Strobl, Z. Phys. **262**, 135 (1973)
40. K. Noba, Y. Kayanuma, K. Nojima, Int. J. Mod. Phys. B **15**, 3908 (2001)
41. N.G. van Kampen, J. Stat. Phys. **54**, 1289 (1989)
42. F.A.B.F. de Moura, Marcelo L. Lyra, Phys. Rev. Lett. **81**, 3735 (1998); Phys. Rev. Lett. **84**, 199 (2000)
43. L.I. Deych, M.V. Erementchouk, A.A. Lisyansky, Phys. Rev. B **67**, 024205 (2003)
44. F. Dominguez-Adame, V.A. Malyshev, F.A.B.F. de Moura, M.L. Lyra, Phys. Rev. Lett. **91**, 197402 (2003)
45. D. Cohen, Phys. Rev. Lett. **67**, 1945 (1991)
46. H. Onishi, S. Miyashita, J. Phys. Soc. Jpn. **72**, 392 (2003)